Received: 28 March 2024 | Accepted: 6 September 2024 | Published online: 9 October 2024

DOI: 10.1002/jeq2.20634

Journal of Environmental Quality

TECHNICAL REPORT

Resource Recovery and Reuse

Biochar captures ammonium and nitrate in easily extractable and strongly retained form without stimulating greenhouse gas emissions during composting

Franziska Busch[1,2] | **Otávio dos Anjos Leal**[1] | **Nina Siebers**[1] | **Nicolas Brüggemann**[1]

[1]Institute of Bio- and Geosciences—Agrosphere (IBG-3), Forschungszentrum Jülich GmbH, Jülich, Germany

[2]Department of Earth System Sciences, Institute of Soil Science, Universität Hamburg, Hamburg, Germany

Correspondence
Otávio dos Anjos Leal, Institute of Bio- and Geosciences—Agrosphere (IBG-3), Forschungszentrum Jülich GmbH, Wilhelm-Johnen-Straße, 52428 Jülich, Germany.
Email: o.dos.anjos.leal@fz-juelich.de

Assigned to Associate Editor Maren Oelbermann.

Funding information
Ministerium für Kultur und Wissenschaft des Landes Nordrhein-Westfalen, Grant/Award Number: 313/323-400-00213

Abstract

During composting of organic waste, nitrogen is lost through gaseous forms and ion leaching. Biochar has been shown to capture mineral nitrogen (N_{min}: NH_4^+ and NO_3^-) from compost, which we hypothesize reduces N_2O formation. However, associating N_{min} captured by biochar with the dynamics of N_2O and other greenhouse gas (GHG) emissions during composting remains unstudied and was the aim of this work. We composted (outdoor for 148 days) together kitchen scraps (43.3% dw, where dw is dry weight), horse manure (40.9% dw), and wheat (*Triticum aestivum* L) straw (15.8% dw) without (Control) or with biochar (Bc, 15% compost dw). The biochar consisted of hardwood and softwood pieces pyrolyzed at 680°C and exhibited 60% of particles with 4–8 mm. We monitored compost GHG (CO_2, CH_4, N_2O) emissions, N_{min} content in compost and biochar particles (sequential extractions), and biochar surface transformations (SEM-EDX and ^{13}C-NMR spectroscopy) along composting. Biochar did not significantly reduce or increase GHG emissions and N_{min} content (mg kg^{-1}) in compost. However, the final NO_3^- amount (g compost $pile^{-1}$) in the Bc treatment was significantly higher (54%) compared to the Control, indicating lower NO_3^- losses. Despite the high aromaticity and minimal contribution of carboxyl C to the biochar structure, biochar retained NH_4^+, mainly in easily extractable form (55%), in the first 2 weeks of composting and mainly in strongly retained form (75%) in the final compost. The NO_3^- content in biochar increased continuously during composting. In the final compost, the NO_3^- content extracted from biochar was 164 (37%, easily extractable), 80 (19%,

Abbreviations: ^{13}C-NMR, ^{13}C-nuclear magnetic resonance; Bc, biochar; Ctrl, control; dw, dry weight; EC, electrical conductivity; Es1, extraction step 1; Es2, extraction step 2; Es3, extraction step 3; GHG, greenhouse gas; GWP, global warming potential; HM, horse manure; K_{av}, plant-available potassium; KS, kitchen scraps; N_{min}, mineral nitrogen; P_{av}, plant-available phosphorus; SSA, specific surface area; TK, total potassium; TN, total nitrogen; TOC, total organic carbon; TOM, total organic matter; TP, total phosphorus; WS, wheat straw.

moderately extractable), and 194 mg NO_3^-–N kg^{-1} (44%, strongly retained). Although N_{min} retention in biochar was not accompanied by lower N_2O emissions, contradicting our hypothesis, we demonstrated the efficacy of biochar to recover N_{min} from organic waste without stimulating GHG emissions.

1 | INTRODUCTION

Agriculture and other land use practices account for approximately 23% of total anthropogenic greenhouse gas (GHG) emissions (Jia et al., 2019). Agricultural intensification and expansion with use of synthetic nitrogen (N) fertilizers has led to major disturbances of the natural N cycle in recent decades (Bouwman et al., 2013; Canadell et al., 2021). According to Jia et al. (2019), in global croplands about 50% of N applied to agricultural fields is not taken up by crops, and N losses in the form of NH_3 volatilization, N_2O and NO emissions, and NO_3^- leaching may occur, with adverse environmental effects (Fowler et al., 2013). Particularly, Germany has failed to keep the N surplus (N input − N harvested) in croplands <100 kg N ha^{-1} $year^{-1}$ and has to make a great effort to meet its target (<70 kg N ha^{-1} $year^{-1}$) by 2030 (UBA, 2020).

Thermophilic composting of organic waste serves to recycle N (Cáceres et al., 2018) and delivers a nutrient-rich, humified, and sanitized compost suitable for agriculture (Castro-Herrera et al., 2022). Nevertheless, nutrient leaching, NH_3 volatilization, and GHG emissions may still occur during composting (Bernal et al., 2009), and co-composting of organic waste with biochar has been proposed to regulate the N cycle by increasing N retention, thus reducing N losses (Sánchez-Monedero et al., 2018).

Biochar is a carbon-rich material produced by anoxic thermal treatment of biomass through pyrolysis (Lehmann et al., 2021). The properties of biochar, including functional groups, great specific surface area (SSA), porosity, and water holding capacity, have been shown to benefit multiple soil properties, regulate the N cycle, and mitigate GHG emissions in croplands (Q. Liu et al., 2018; Schmidt et al., 2021). In compost, biochar may favor nutrient retention, aerobic microbial activity, and compost maturation, while reducing GHG emissions, especially CH_4 and N_2O (Awasthi et al., 2017; Castro Herrera et al., 2023; Q. Wang et al., 2018), which have a global warming potential (GWP) 27 and 273 times higher than CO_2, respectively (IPCC, 2021). Particularly, co-composting of biochar and organic waste has gained increasing attention as it recovers NH_4^+ and mainly NO_3^- from compost piles, as nitrification is intrinsic to aerobic composting (Ajibade et al., 2023; Cáceres et al., 2018). Compared to anaerobic composting, aerobic composting may demand more man or electrical power to turn and oxygenate the piles, depending on the pile scale, but it has the advantage of delivering compost with greater maturation in a shorter composting time (Yang et al., 2019), likely with lower GHG emissions (N. Wang et al., 2024; Yuan et al., 2016).

During composting, NO_3^--rich water is trapped in biochar pores, which are subsequently closed by the formation of organo-mineral layers (Joseph et al., 2018). This was verified through increased recovery of NO_3^- from co-composted biochar particles after successive extractions of (plant-available and unavailable) NO_3^- (Hagemann, Joseph, et al., 2017; Hagemann, Kammann, et al., 2017; Kammann et al., 2015). Similar findings were reported for soil-aged biochar (Haider et al., 2020) and for NO_3^- removal from water using biochar as adsorbent (Loganathan et al., 2013).

Together, the capture of NH_4^+ and NO_3^- and the improvement of compost aeration by biochar may reduce the pool of mineral nitrogen (N_{min}) available to nitrifying bacteria and archaea, and the activity of denitrifying bacteria and fungi in compost (He et al., 2017; Kammann et al., 2015; Steiner et al., 2010), likely reducing N_2O losses. Biochar-induced mitigation of GHG emissions during composting has been studied by optimizing the amount of biochar, feedstock, pyrolysis temperature, and particle size (Nguyen et al., 2022; Sánchez-Monedero et al., 2018; Yin et al., 2021). Nevertheless, studies of co-composting biochar have not simultaneously assessed the degree of availability and the amount of N_{min} retained by biochar particles in relation to temporal N_2O dynamics. For instance, a statistical review by Firmino and Trémier (2023) emphasized that commonly analyzed biochar parameters explained only 45% of mitigation of N loss from compost, and that understanding the relationship between N retention by biochar and compost N_2O emissions remains critical to optimizing this process.

Most studies on biochar co-composting focus on cattle, chicken, swine, sheep, or human manure (Akdeniz et al., 2019; Castro-Herrera et al., 2023; Zhou et al., 2023), while horse manure (HM) is understudied. Particularly, the German state of North Rhine-Westphalia is known for concentrating horse farms and for being agriculturally active. For proper composting, HM can be mixed with other available organic wastes, such as kitchen scraps (KS), and co-composted with biochar, finally returning to agriculture as N-enriched compost. Given the above considerations, we aimed to use biochar to recover N during co-composting of these valuable organic wastes and to investigate the relationship between N_{min} forms and availability in biochar particles and GHG emissions

during composting. We hypothesized that biochar retains substantial amounts of NH_4^+ and NO_3^-, which is accompanied by a reduction of N_2O emissions during composting.

2 | MATERIALS AND METHODS

2.1 | Biochar characterization

The feedstock (hardwood and softwood in the form of wood chips) was pyrolyzed at 680°C with a residence time of 30 min (AWN Abfallwirtschaft). The characteristics of the resulting biochar are displayed in Table 1. These analyses were conducted by Eurofins Umwelt Ost GmbH (Bobritzsch-Hilbersdorf) according to the European Biochar Foundation (2012), and the biochar fulfilled the requirements of the European Biochar Certificate.

2.2 | Experimental design

The compost experiment was conducted outdoors at Forschungszentrum Jülich GmbH (FZJ) (Figure S1), Jülich, Germany, for 148 days. The feedstocks used were KS, HM, and wheat (*Triticum aestivum* L) straw (WS) (Table 1). The KS, provided by Burgmühle Salate und Gemüse GmbH, consisted of chopped cabbage, apple peel, eggplant, carrot, tomatoes, onions, lemons, and lettuce. The HM was obtained from a local ranch (Stütgerhof), and the WS was purchased online (Wilms Lohnunternehmen e.K.).

The KS, HS, and WS were thoroughly mixed without any pre-treatment using compost forks and evenly distributed into six plug-in wooden boxes (0.85 m × 0.85 m × 1.20 m height). The initial weight of feedstock mix per box was 276 kg (71 kg dw, where dw is dry weight) and the initial pile height was 105 cm (480.3 kg m^{-3} bulk density). In three of the boxes, the biochar was mixed with the feedstocks (biochar [Bc] treatment). The three other boxes without biochar represented the control (Ctrl). Each Bc box received 12.7 kg (10.7 kg dw) of biochar, equivalent to 15% of compost dw, meeting proper biochar co-composting recommendations (Sánchez-Monedero et al., 2018; Yin et al., 2021). The boxes were covered with a compost fleece (TopTex 200 g m^{-2}, dienatur) to prevent rain infiltrating the compost and excessive compost moisture loss. As composting started during hot and dry summer, piles were watered on days 34, 37, 41, and 78 to keep proper compost moisture, 40%–65% (Rynk et al., 1992). As the experiment entered a rainy period, the boxes were covered with a pond liner to prevent uncontrolled rainwater intrusion into the compost. Compost insulation was promoted by installing WS on the outer sides of the boxes. Piles were turned using compost forks on days 15, 41, 77, and 108 to enhance compost aeration and microbial activity, and to prevent compaction.

Core Ideas

- Biochar particles retained NH_4^+ in an early and NO_3^- in a later phase of composting.
- Highly aromatic biochar captured NH_4^+ and NO_3^- in easily extractable and strongly retained forms.
- Compost amended with biochar had a higher final NO_3^- content without stimulating greenhouse gas emissions.

2.3 | Sampling of compost and preparation of compost samples

Compost was sampled on days 1, 8, 15, 29, 43, 57, 71, 84, 96, 104, 126, 139, and 148. Each sample consisted of three sub-samples taken at different depths at the edge, corners, and center of the pile. Fresh and frozen samples were ground < 5mm using a hand blender. Fresh samples were used to monitor compost moisture content (MC) and for the germination index (GI) test. Frozen samples were stored on the day of sampling and kept at −20°C until analysis of pH, electrical conductivity (EC), N_{min}, plant-available phosphorus (P_{av}), and plant-available potassium (K_{av}). Dried samples were ball-milled for determination of total nitrogen (TN), total organic carbon (TOC), total organic matter (TOM), total phosphorus (TP), and total potassium (TK) content. Details on GI, P_{av}, K_{av}, TP, and TK are available in the Supporting Information.

2.4 | Compost parameters

Compost temperature was measured at 18 points within the pile (at two different depths) using a thermometer equipped with a 64-cm-long stainless-steel probe (G1700, GTF 40T-620, Greisinger) and monitored daily until day 38, three times per week until day 66, weekly until day 99, and on days 110, 127, and 148. Ambient air temperature was provided by the weather station on FZJ campus.

The MC of compost samples and biochar particles was determined gravimetrically (24 h at 105°C). Compost pH was measured with a glass electrode (WTW Multi 3630 IDS, SenTix940, Xylem Analytics) in a 1:10 (w/v) deionized water extract. Compost EC was determined in deionized water extract (1:10, w/v) after 1 h shaking (250 rpm), 15 min centrifugation (3500 rpm), and filtration (Whatman V2 filter paper) using a conductivity meter (WTW Multi 3630 IDS, TetraCon325, Xylem Analytics). Compost TN and TOC concentration were measured with an elemental analyzer (Flash EA 2000 coupled with a Delta V Plus, Thermo Fisher Scientific), and TOM content was determined by measuring weight

TABLE 1 Characterization of biochar and kitchen scraps (KS), horse manure (HM), and wheat straw (WS) used in the compost experiment.

Variable	Biochar	Variable	KS	HM	WS
pH $CaCl_2$	8.5	Total fresh weight, kg	1076.6	503.3	74.5
Ash (550°C), %	5.1	Dry weight (dw) rate, %	43.3	40.9	15.8
K (K_2O), % (dw)	0.58	Moisture (by weight), %	82.5	66.6	7.8
Ca (CaO), % (dw)	1.9	TOC, g kg^{-1}	375.7 ± 1.2	396.1 ± 1.3	423.4 ± 1.3
Mg (MgO), % (dw)	0.13	TN, g kg^{-1}	33.3 ± 0.1	14.6 ± 0.1	5.8 ± 0
P (P_2O_5), % (dw)	0.07	C:N	11.3 ± 0.1	27.2 ± 0.3	73.3 ± 0.4
Organic C, % dw	89.7	NH_4^+–N, mg kg^{-1}	205.4 ± 8.9	15.2 ± 0.9	Nd
Total N, % (dw)	0.72	NO_3^-–N, mg kg^{-1}	0.7 ± 0	6.8 ± 0.2	Nd
H/C_{org} molar ratio	0.17	NO_2^-–N, mg kg^{-1}	2.64 ± 0.1	0.5 ± 0	Nd
O/C molar ratio	0.034	Available P, mg kg^{-1}	16.9 ± 1.5	476.1 ± 50.2	Nd
PAH, mg kg^{-1}	3.9	Available K, mg kg^{-1}	163.2 ± 12.2	1850.3 ± 278.9	Nd
SSA, m^2 g^{-1}	421	Total P, mg kg^{-1}	5133.3 ± 152.8	4356.7 ± 135.8	750 ± 10.0
WHC, g 100 g^{-1}	238	Total K, mg kg^{-1}	45,696.7 ± 1643.2	18,366.7 ± 378.6	6490.0 ± 30.0
Particles >8 mm[a], %	26.2	Total Ca, mg kg^{-1}	6373.3 ± 140.5	5882.0 ± 249.9	3326.3 ± 98.1
Particles 8–4 mm, %	59.8	Total Mg, mg kg^{-1}	2003.3 ± 32.1	2433.3 ± 98.7	713.3 ± 15.3
Particles 4–2 mm, %	17.4	Total Fe, mg kg^{-1}	594.0 ± 49.3	1560 ± 98.5	1693.3 ± 102.6
Particles <2, %	14.6	Total Mn, mg kg^{-1}	32.8 ± 1.0	407.7 ± 26.2	40.7 ± 0.6

Note: For KS, HM, and WS, values are average ± standard error ($n = 3$).

Abbreviations: Nd, not detectable; PAH, polycyclic aromatic hydrocarbons; SSA, specific surface area; TN, total nitrogen; TOC, total organic carbon; WHC, water holding capacity.

[a]Complete distribution in Figure S2.

loss after 6-h ignition in a muffle furnace at 550°C. These analyses were conducted according to FAO (2008).

2.5 | N_{min} in compost and biochar particles

Compost N_{min} was extracted with 0.01 mol L^{-1} $CaCl_2$ (1:10 w/v) after 2-h shaking (200 rpm), 15-min centrifugation (3500 rpm), and filtration (0.45 µm polypropylene syringe filter, Dissolution Accessories) (VDLUFA, 2014). For N_{min} extraction from biochar particles (adapted from Haider et al., 2016), 4 g of biochar particles of different sizes (3–10 mm) were carefully picked manually with forceps from frozen compost samples without any compost residues, similar to Kammann et al. (2015), and placed into 50-mL centrifuge tubes, followed by extraction step 1 (Es1: easily extractable): 1 h shaking (200 rpm) in deionized water (1:10, w/v); extraction step 2 (Es2: moderately extractable): 1 h shaking (200 rpm) in 2 mol L^{-1} KCl (1:10, w/v); and extraction step 3 (Es3: strongly retained): shaking in 2 mol L^{-1} KCl in a water bath for 24 h (including water bath heating at 80°C for 8 h). After each extraction step, the entire solution was extracted with a needle (0.6 mm) and filtered (0.45 µm).

Compost and biochar-extracted NO_3^- concentration was determined by ion chromatography (IC850/IC 930 Metrohm) and NH_4^+ and NO_2^- concentrations were determined by Continuous Flow Analysis (Alliance Instruments). The dw of the compost pile was calculated according to Schäfer (2020) (Supporting Information, p. S3) to estimate the nutrient content per compost pile.

2.6 | CO_2, N_2O, and CH_4 measurements

Gas fluxes were measured three times per week until day 67, twice per week until day 81, and on days 85, 92, 99, 110, 127, and 148 using the static chamber-based method. Four cylindrical PVC tubes (25 cm height and 11-cm diameter) were inserted in each compost pile. The tubes were sealed with a screwable PVC lid equipped with a rubber gasket. Each lid was equipped with one septum for syringe gas sampling and two cable entries (2–7 mm), one for temperature measurement in the chamber headspace, and one for a vent tube (1/8″) used for pressure equilibration inside the chamber during gas sampling. Gas samples were taken from the headspace of each of the four chambers (totaling 10–30 mL) at four time points (intervals ranging from 5 to 45 min) using a 50-mL polypropylene syringe, transferred to 20-mL pre-evacuated gas chromatography vials (crimp neck vial Macherey-Nagel), and analyzed for CO_2, CH_4, and N_2O in a gas chromatograph equipped with electron capture detector (ECD) and flame ionization detector (FID) (Clarus 580, PerkinElmer). Gas fluxes

were calculated according to Equation 1:

$$GHG_{flux} = \frac{S}{1,000,000} \times \frac{PV}{RT} \times \frac{M}{A} \quad (1)$$

where S is the slope of gas concentration increase with time (ppm h^{-1}), to convert ppm (μL L^{-1}) to L L^{-1}, S is divided by 1,000,000, P is the atmospheric pressure in the chamber (1 atm), V is the chamber headspace (L), R is the universal gas constant (0.0831446 atm L mol^{-1} K^{-1}), T is the average chamber temperature (K), M is the molar mass of C or N (g mol^{-1}), and A is the basal area of the chamber (m^2). The slope (S) was set to zero if $R^2 < 0.81$. Compost GWP calculation is detailed in Supporting Information (p. S3).

2.7 | SEM-EDX and ^{13}C-NMR spectroscopy analysis of biochar

The surface morphology and elemental composition of the original biochar (Bc0) and biochar co-composted for 148 days (Bc148) were analyzed using scanning electron microscopy (SEM) equipped to an energy dispersive X-ray spectrometer (EDX). Bc0, biochar co-composted for 77 days (Bc77), and Bc148 were subjected to carbon-13 nuclear magnetic resonance (^{13}C-NMR) spectroscopy to investigate composting-induced shifts in the chemical structure of biochar. Details on SEM-EDX and ^{13}C-NMR methods are displayed in Supporting Information (p. S4 and S5).

2.8 | Statistical analysis

The data are presented as mean ± standard error (SE) ($n = 3$). The means of Ctrl and Bc and the elemental composition of Bc0 and Bc148 were compared by t-test ($p < 0.05$). Data analysis and visualization were conducted with the RStudio (Version 4.2.3 RStudio, PBC).

3 | RESULTS

3.1 | Control parameters

Both Ctrl and Bc underwent four composting phases: mesophilic phase I (1 day < 45°C), thermophilic phase (8 days ≥45°C), mesophilic phase II (66 days < 45°C), and maturation phase (64 days; ambient temperatures) (Figure 1). Biochar did not affect compost temperature.

Initial compost MC decreased from 74.9% (Ctrl) and 74.2% (Bc) to final values of 54.2% (Ctrl) and 55.5% (Bc), with the most abrupt decrease noticed within the thermophilic phase (Figure 2a). These initial MC values were above the recommended range (40%–65%), likely due to the MC of KS (91.8%). When composting entered a dry summer period, manual watering compensated for evaporation losses, and compost MC remained within the recommended range (Figure 2a) without significant effects of biochar.

Initial compost pH (9.5) decreased gradually during composting to final values of 8.8 (Ctrl) and 8.9 (Bc), and significant differences occurred only on days 84 and 104, where pH was greater in Bc compared to Ctrl (Figure 2b). Initial compost EC (1.8 mS cm^{-1}) tended to increase over composting days in Ctrl and Bc (Figure 2c). Interestingly, EC decreased from 3.3 to 2.7 mS cm^{-1} (Ctrl) and from 2.7 to 1.9 mS cm^{-1} (Bc) between days 57 and 84, and afterward increased to 3.5 mS cm^{-1} (Ctrl) and 2.9 mS cm^{-1} (Bc) in the final compost. From day 96 to 148 (end), EC was significantly higher (21%) in Ctrl compared to Bc (Figure 2c).

Initial compost C:N ratio (24) dropped to 15 (Ctrl) and 18 (Bc) during the first week of composting but did not differ statistically (Figure 2d). In Ctrl, the C:N ratio decreased pronouncedly within the thermophilic phase and thereafter steadily until day 148 (11.1) (Figure 2d). In contrast, the C:N ratio in Bc increased to 27 on day 15 and remained stable until day 148 (24) (Figure 2d). During this time, the C:N ratio in Bc was statistically higher by 1.7- to 2.2-fold compared to Ctrl (Figure 2d).

Decrease of TOM during composting was more evident in Ctrl (82.3%–72.4%) than in Bc (82.5%–79.3%) (Figure 2e). In Ctrl, TOM decreased remarkably until the beginning of the mesophilic phase II, whereas in Bc, the greatest TOM decrease occurred at the beginning of the thermophilic phase and remained practically unaltered until compost finalization (Figure 2e). Except for days 1, 8, and 71 (no statistical differences), TOM was statistically higher in Bc (Figure 2e).

On day 1, TOC in Ctrl (40.2%) and Bc (41.3%) did not differ statistically (Figure 2f). In Ctrl, TOC decreased significantly to 35.6% on day 148, whereas in Bc TOC increased, mainly until the beginning of mesophilic phase II, and reached 55% on day 148 (Figure 2f). From day 15 onward, compost TOC was 34%–55% significantly higher in Bc compared to Ctrl (Figure 2f).

3.2 | Nitrogen dynamics in compost

The TN in Ctrl and Bc did not differ statistically until day 15, afterward TN increased up to 3.2% in Ctrl and 2.3% in Bc and was significantly higher in Ctrl, except on day 71 (Figure 3a). On the contrary, TN (g $pile^{-1}$) in Ctrl and Bc did not differ statistically, except for the higher TN in Bc on day 7 (Figure 3b).

Compost NH_4^+ contents peaked on day 1 at 114.9 (Ctrl) and 118.2 mg N kg^{-1} (Bc), decreased continuously and were lowest on day 148 (Ctrl 31.5 and Bc 29.0 mg N kg^{-1}). Such

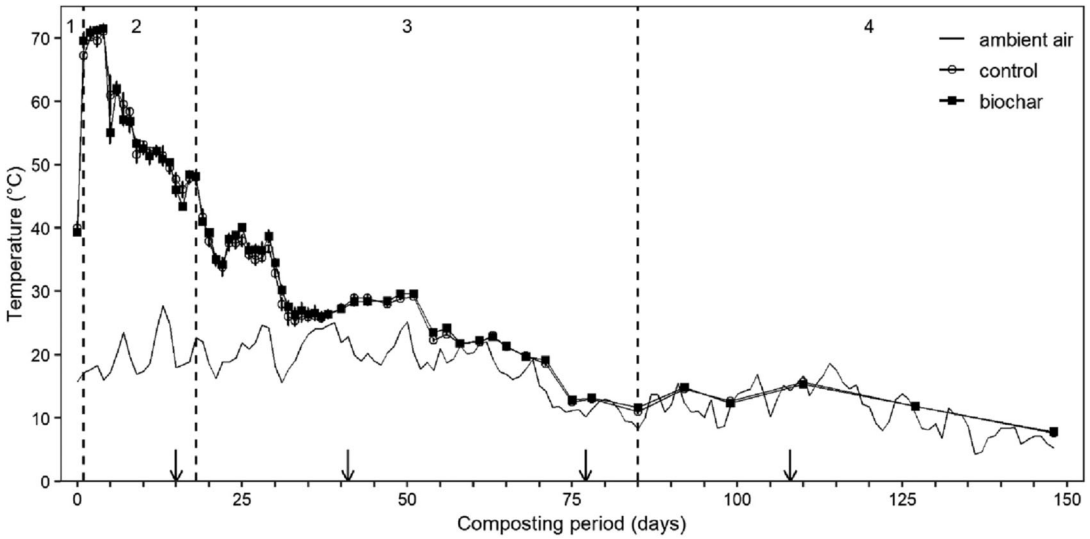

FIGURE 1 Temperature of compost treatments and ambient air over the composting period. Values are reported as mean ($n = 3$) and error bars show standard error. Dashed vertical lines indicate the following composting phases: (1) mesophilic phase I (<45°C), (2) thermophilic phase (≥45°C), (3) mesophilic phase II (<45°C), and (4) maturation phase (close to ambient temperature). Arrows indicate compost pile turning events.

decline was more pronounced in the thermophilic phase, and after a transient increase on day 29, it declined again continuously until the end of composting in both treatments (Figure 3c). During composting, NH_4^+ contents (Figure 3c) and amount per pile (Figure 3d) in Ctrl and Bc did not differ significantly.

In both treatments, detectable NO_3^- contents occurred only from day 43 onward (Figure 3e), when NO_3^- contents continued to rise steadily until day 148 (Ctrl 256.1 and Bc 261.5 mg N kg^{-1}), without significant differences (Figure 3e). Interestingly, the NO_3^- amount in Bc (g N $pile^{-1}$) was significantly higher than in Ctrl on days 96, 136, and 148 (54.2% higher) (Figure 3f).

3.3 | Nitrogen dynamics in biochar particles

The highest NH_4^+ contents in biochar particles were extracted on day 1 at Es1, Es2, and Es3 (116.8, 50.3, and 43.4 mg N kg^{-1}, respectively) (Figure 4a). Throughout composting, NH_4^+ contents in Es1 and Es2 tended to decrease until 8.4 mg N kg^{-1} or were below detection limit, respectively, while that in Es3 remained between 17.6 and 25.3 mg N kg^{-1} (Figure 4a). At the beginning of composting, 55.2% of the NH_4^+ content in biochar was extracted in Es1, whereas in the final compost, 74.7% was extracted in Es3 (Figure 4b).

The NO_3^- contents extracted from biochar were negligible until day 29 (Figure 4e). From day 43 to 148, NO_3^- contents increased progressively, mainly in Es1 and Es3 (Figure 4e). In the final compost, the NO_3^- content in Es1, Es2, and Es3 (164.4, 80.0, and 194.3 mg N kg^{-1}), corresponded to 37%, 19%, and 44% of total NO_3^-–N in biochar, respectively (Figure 4f). This proportion remained practically unaltered since day 84. On day 148, the sum of NH_4^+ and NO_3^- content in biochar (471.4 mg N kg^{-1}) was 37% and 46% extracted in Es1 and Es3, respectively.

3.4 | Temporal dynamics of CO_2, CH_4, and N_2O emissions

The highest CO_2 emissions occurred on day 1 in Ctrl and Bc, 11,905 and 13,373 mg CO_2-C m^{-2} h^{-1}, respectively, without significant differences (Figure 5a). A second peak occurred on day 16 (after turning piles on day 15), which was 31% higher in Ctrl (8041 mg CO_2-C m^{-2} h^{-1}) compared to Bc (Figure 5a). Subsequently, CO_2 emissions decreased gradually. Following the second pile turning (day 41), CO_2 emissions slightly increased on day 42, more in Ctrl than in Bc (1390 and 1068 mg CO_2-C m^{-2} h^{-1}, respectively), but without significant difference (Figure 5a). Thereafter, CO_2 emissions stabilized despite pile turnings (days 77 and 108) and reached 29 and 22 mg CO_2-C m^{-2} h^{-1} in Ctrl and Bc, respectively, on day 148 (Figure 5a). Cumulative CO_2 emissions averaged 4016 and 3706 g CO_2-C m^{-2} in Ctrl and Bc, respectively, without significant difference (Figure S3a).

Similar patterns of CH_4 emissions were observed in Ctrl and Bc, which exhibited highest emission peaks of 4883 on day 5 and 7944 μg CH_4-C m^{-2} h^{-1} on day 19 in Ctrl and Bc, respectively (Figure 5b). From day 58, no significant CH_4 emissions were detected (Figure 5b). Cumulative CH_4 emissions in Ctrl and Bc averaged 2171 and 3332 mg CH_4-C m^{-2}, respectively, without statistical difference (Figure S3b).

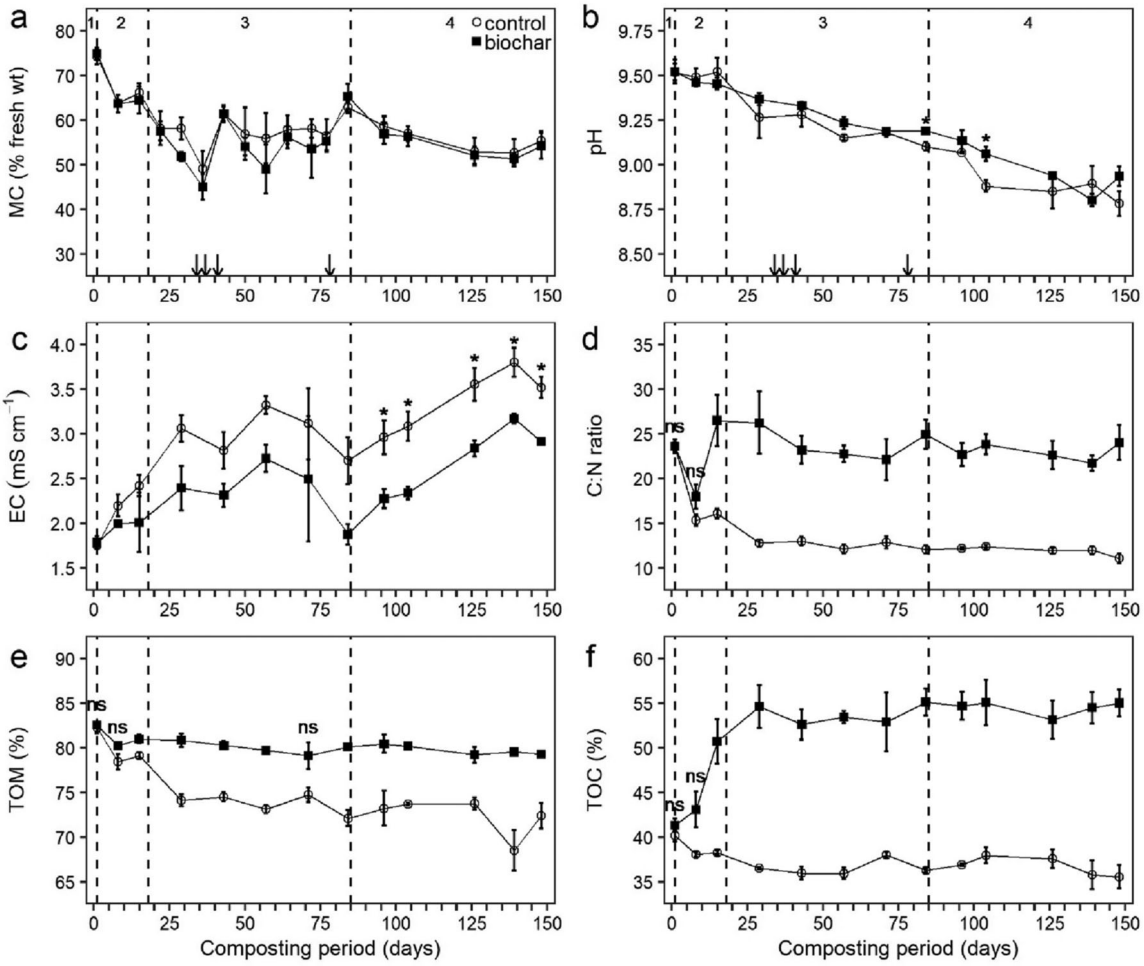

FIGURE 2 Control parameters during the composting process: (a) moisture content (MC), (b) pH, (c) electrical conductivity (EC), (d) C:N ratio, (e) total organic matter (TOM), and (f) total organic carbon (TOC). Values are means ($n = 3$) and error bars are standard error. Arrows indicate watering events of compost piles. Asterisks (*) indicate significant ($p < 0.05$) difference between treatments within the sampling date. In (d), ns indicates no significant difference, otherwise control and biochar treatments differed statistically ($p < 0.05$). Dashed vertical lines indicate the following composting phases: (1) mesophilic phase I (<45°C), (2) thermophilic phase (≥45°C), (3) mesophilic phase II (<45°C), and (4) maturation phase (close to ambient temperature).

On day 2, N_2O emissions in Ctrl and Bc were 1878 and 2114 μg N_2O-N m^{-2} h^{-1}, respectively, and abruptly decreased until day 14 (Figure 5c). After the first pile turning (day 15), N_2O emissions increased again, without significant differences between treatments (Figure 5c). The second peak of N_2O emissions in Ctrl and Bc (3595 and 1504 μg N_2O-N m^{-2} h^{-1}, respectively) occurred after the second pile turning on day 42, without statistical difference (Figure 5c). Subsequently, N_2O emissions remained low (Ctrl 33 and Bc 13 μg N_2O-N m^{-2} h^{-1}), despite piles turning on days 77 and 108. Cumulative N_2O emissions in Bc (563 mg N_2O-N m^{-2}) were 21% lower but did not differ from that of Ctrl (Figure S3c).

Total GHG emissions in Ctrl and Bc were 4121 and 3804 g CO_2-C-eq m^{-2}, respectively, and although GWP was 8% lower in Bc, treatments did not differ significantly (Figure S3d).

3.5 | ^{13}C-NMR spectra of original and composted biochar

The ^{13}C-NMR spectra of original and co-composted biochar were similar and largely dominated by aryl C (Figure 6). The contribution (%) of aryl C to the total ^{13}C intensity gradually decreased with composting time as follows: Bc0 > Bc77 > Bc148 (Figure 6). Oppositely, the alkyl C contribution gradually increased with composing time: Bc0 < Bc77 < Bc148 (Figure 6). As a result of the shifts in aryl C and alkyl C spectral regions caused by the composting of biochar, the aromaticity index (ArI) of biochar decreased considerably with composting: Bc0 > Bc77 > Bc148 (Figure 6). Although the contribution of carboxyl C, O/N-aryl C, O-alkyl C, and N-alkyl C tended to increase as a

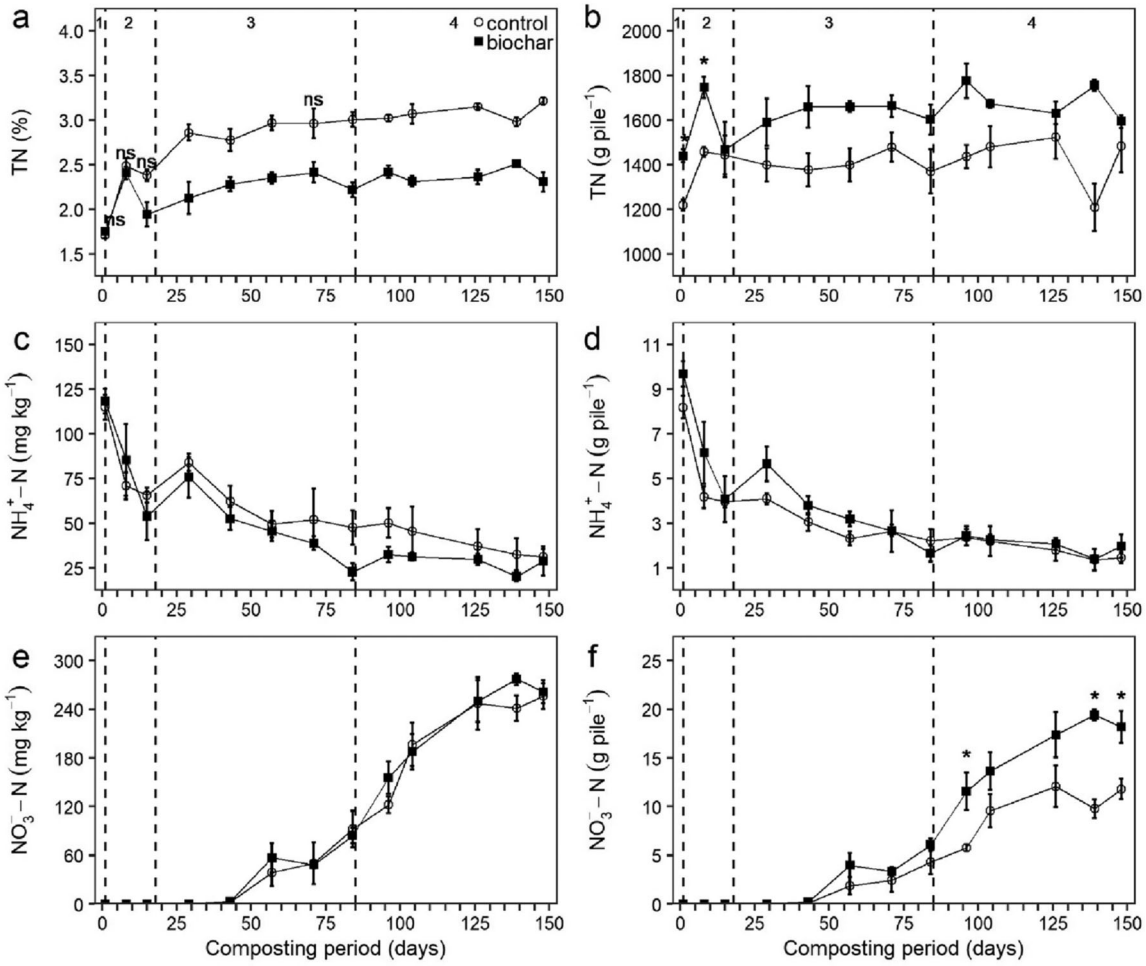

FIGURE 3 Compost total nitrogen (TN) concentration (a) and amount per compost pile (b), ammonium (NH_4^+–N) content (c) and amount per compost pile (d), nitrate (NO_3^-–N) content (e), and amount per compost pile (f). Values are means ($n = 3$) and error bars are standard error. Dashed vertical lines indicate the following composting phases: (1) mesophilic phase I (<45°C), (2) thermophilic phase (≥45°C), (3) mesophilic phase II (<45°C), and (4) maturation phase (close to ambient temperature). Asterisks (*) indicate significant ($p < 0.05$) differences between treatments within the sampling date.

signal of biochar aging through composting, these changes were minimal (<1.2%) (Figure 6).

4 | DISCUSSION

4.1 | Composting phases and control parameters

The high temperatures at early composting are typical of the thermophilic phase, indicate high microbial activity and decomposition of easily degradable organic compounds (Rynk et al.,1992), and met the criteria of the German Biowaste Ordinance (BIOAbfV 2022). Consequently, Ctrl and Bc are considered sanitized and suitable for agriculture (Bernal et al., 2009). Biochar is known to enhance compost temperatures through improved oxygenation and microbial activity (Kammann et al., 2016; N. Liu et al., 2017), but biochar did not affect compost temperature in our study, agreeing with Zhang et al. (2020). This is consistent with the typical low availability of easily biodegradable C in biochar, which would probably increase microbial activity and temperature in compost. Such deviation of our findings compared to these studies may be attributed to compost oxygenation provided by using 15.8% WS in our compost, as also found by Castro-Herrera et al. (2022) for composting human excreta with and without biochar. In addition, biochar did not affect compost MC, suggesting that the role of biochar as a dry bulking (Castro-Herrera et al., 2022; N. Liu et al., 2017) or a porous-water retention agent (Prost et al., 2013; López-Cano et al., 2016) was balanced in our compost.

The decline of pH in Ctrl and Bc during composting is possibly linked to nitrification and release of H^+ in compost (Sánchez-Monedero et al., 2001). This is suggested by the

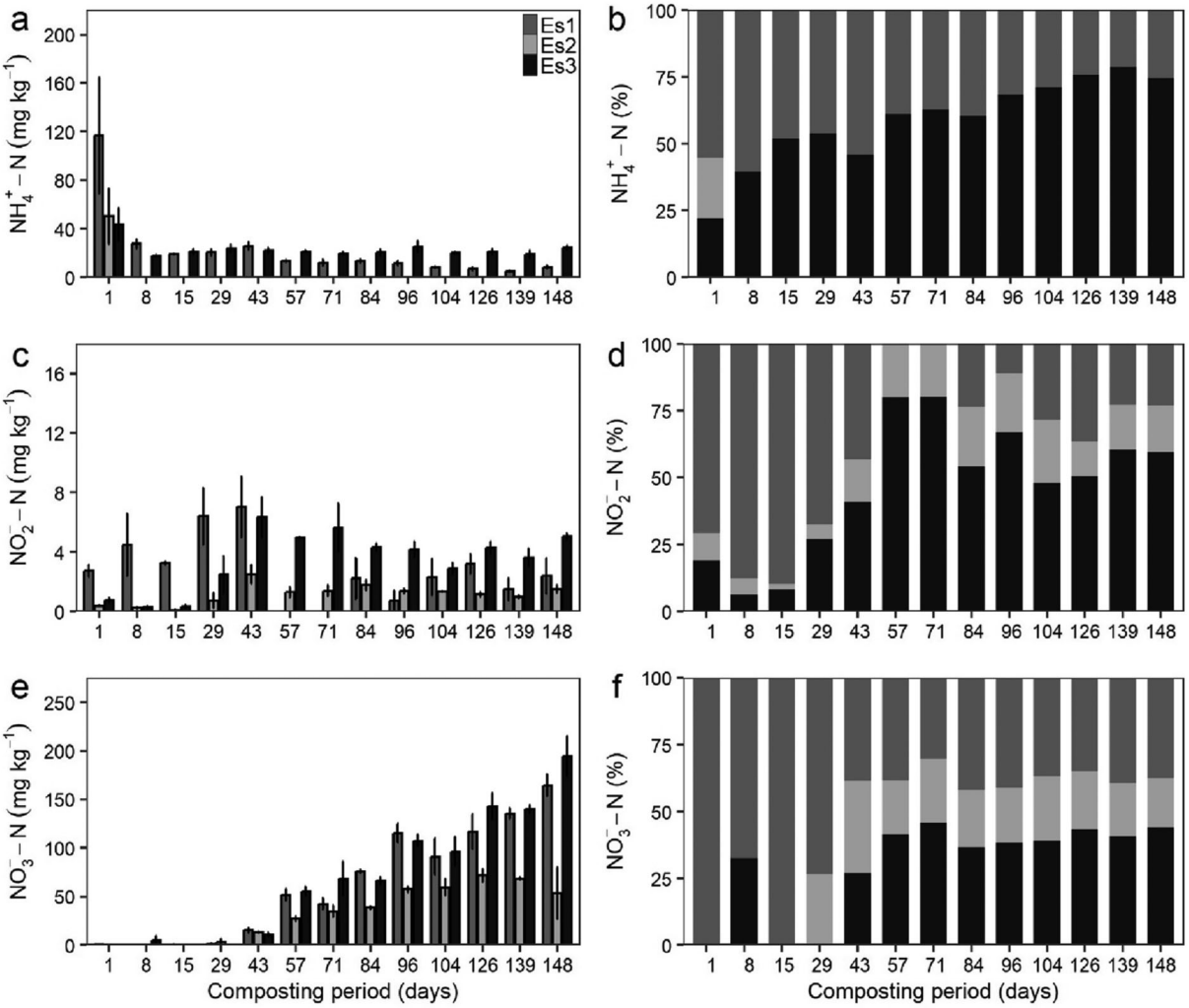

FIGURE 4 Content and proportion of ammonium (NH_4^+–N) (a and b) nitrite (NO_2^-–N) (c and d), and nitrate (NO_3^-–N) (e and f) extracted from biochar particles after extraction step 1 (Es1): 1 h shaking (200 rpm) in deionized water (1:10, w/v); step 2 (Es2): 1 h shaking (200 rpm) in 2 mol L^{-1} KCl (1:10, w/v); and step 3 (Es3): shaking in 2 mol L^{-1} KCl in a water bath for 24 h (including water bath heating at 80°C for 8 h). Values are means ($n = 3$) and error bars are standard error.

simultaneous steady decline in NH_4^+ and increase in NO_3^- content during composting. The initial pH of compost (9.5) exceeded values reported in other studies (Awasthi et al., 2017; R. Li et al., 2015; López-Cano et al., 2016; Q. Wang et al., 2018), and biochar did not induce compost alkalinization in the thermophilic phase in our experiment, contracting other studies (Castro-Herrera et al., 2022; R. Li et al., 2015; Q. Wang et al., 2018; Zhang et al., 2020). This divergence might be attributed to the lower pH of biochar in our experiment (8.5) compared to the biochar (pH > 10) used in the referred studies. Moreover, the initial pH of our compost (9.5) was already higher than that of the biochar (8.5), likely preventing biochar-induced compost alkalinization.

The increase in compost EC in Ctrl and Bc (Figure 2c) is apparently associated with nitrification and OM mineralization, as suggested by a decline of TOM (Figure 2e), which is generally associated with the release of salts (Maheshwari et al., 2014). The TOM decline in Bc is attenuated because biochar recalcitrance may mask the decomposition of the fresh compost feedstocks. The lower EC of Bc compared to Ctrl from day 96 to 148 may be associated to the retention of ions by the biochar, thereby reducing soluble salt concentrations in compost, and moreover to the greater loss of compost mass in Ctrl compared to Bc, resulting in higher nutrient concentrations and consequently higher EC values in Ctrl (R. Li et al., 2015). The ^{13}C-NMR spectra of biochar revealed its minimal increments with carboxyl C after composting (Figure 6), confirming its resistance to microbial attack. De la Rosa et al. (2018) reported shifts of similar nature and magnitude in the ^{13}C-NMR spectra of biochar aged in soil for 120 days. The abrupt decline of EC in both treatments on day 84 coincides with a manual watering of piles on day 78, which may have diluted salts in the compost, supporting increase in compost MC on day 84. The EC of mature final composts

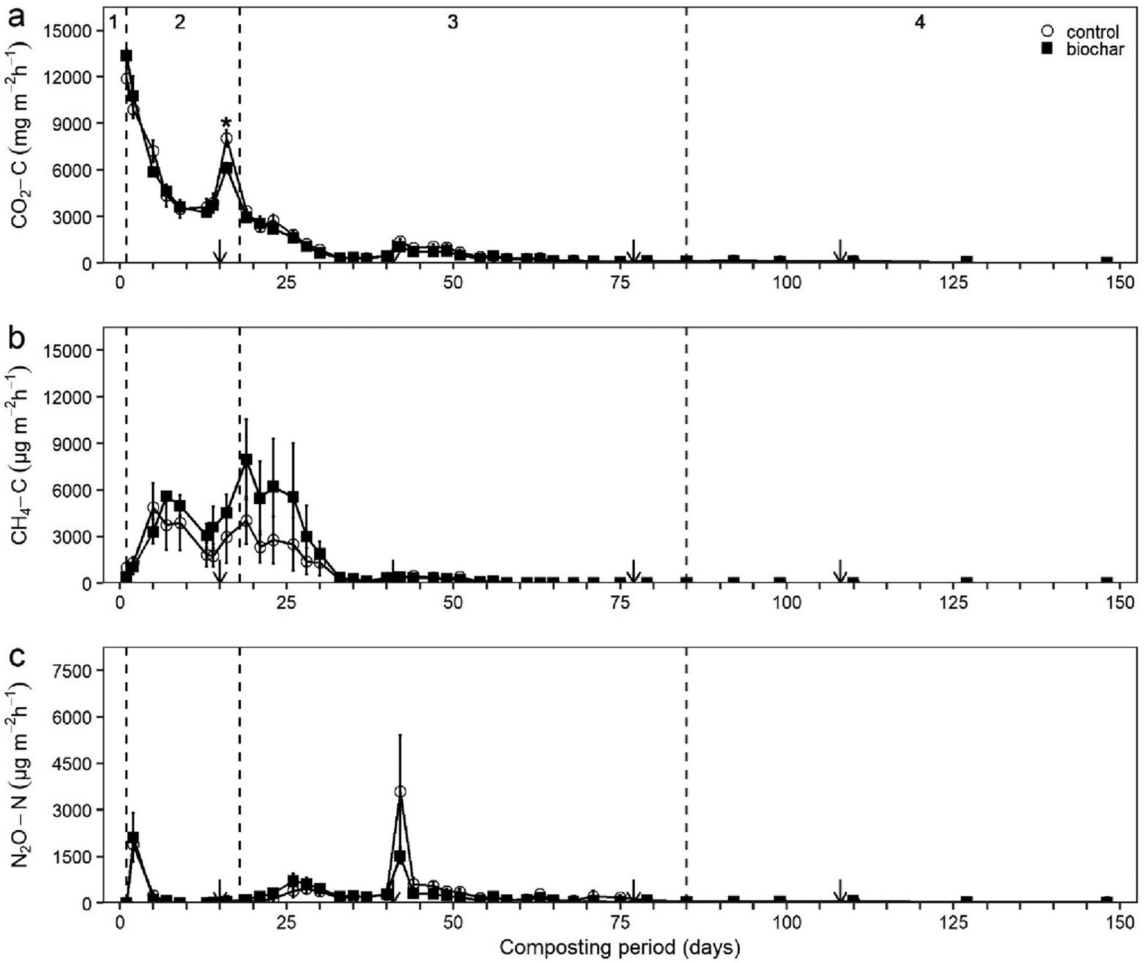

FIGURE 5 CO_2 (a), CH_4 (b), and N_2O (c) emissions over the course of composting. Values are means ($n = 3$) and error bars are standard error. Arrows indicate pile-turning events. *Significant at $p < 0.05$.

was <4 mS cm^{-1}, indicating their suitability for plant growth (Lasaridi et al., 2006).

The higher C:N ratio in Bc compared to Ctrl may be attributed to the stability of biochar with high C content and its increasing concentration in the pile as side effect of compost feedstocks decomposition. For instance, the final C:N ratio of Ctrl (11.1) reached the ideal range of mature compost. In Bc, the final C:N ratio was 24, and compost maturation was confirmed by the GI and other maturity indicators (Supporting Information, pages S10 and S11). Khan et al. (2014) reported similar effects of biochar on compost C:N ratio dynamics.

The increase and decrease in TOC (%) observed in Bc and Ctrl during composting, respectively, reflect proper composting conditions and OM decomposition, and the concentration of biochar in Bc compost piles with composting time. This is explained by the predominance of condensed aromatic structures in the original biochar (indicated by aryl-C = 84.1%, Figure 6), in agreement with its H/C (0.17) and O/C (0.03) molar ratios (Table 1) indicative of high aromaticity, which confer high resistance to biochar against microbial decomposition in compost (Fischer & Glaser, 2012; Hagemann et al., 2018).

4.2 | Nitrogen dynamics in compost

Mineralization of OM releases NH_4^+ as reflected by the high NH_4^+ contents in initial Ctrl and Bc compost. The rapid decline in NH_4^+content during the thermophilic phase without a proportional increase in NO_3^- may indicate NH_3 volatilization, which is favored by compost temperatures >45˚C and pH >9 due to NH_4^+ deprotonation (Beck-Friis et al., 2001). On the other side, easily decomposable feedstocks as KS may favor NH_4^+ immobilization by microorganisms, thereby reducing N-losses by NH_3 volatilization (Bernal et al., 2009). Overall, the similar pH, temperature, MC, NH_4^+, and NO_3^- content in Ctrl and Bc compost, coupled with the strong retention of NH_4^+ by biochar particles in the thermophilic phase, suggest that, if relevant NH_3 volatilization occurred, it may have been similar in Ctrl and

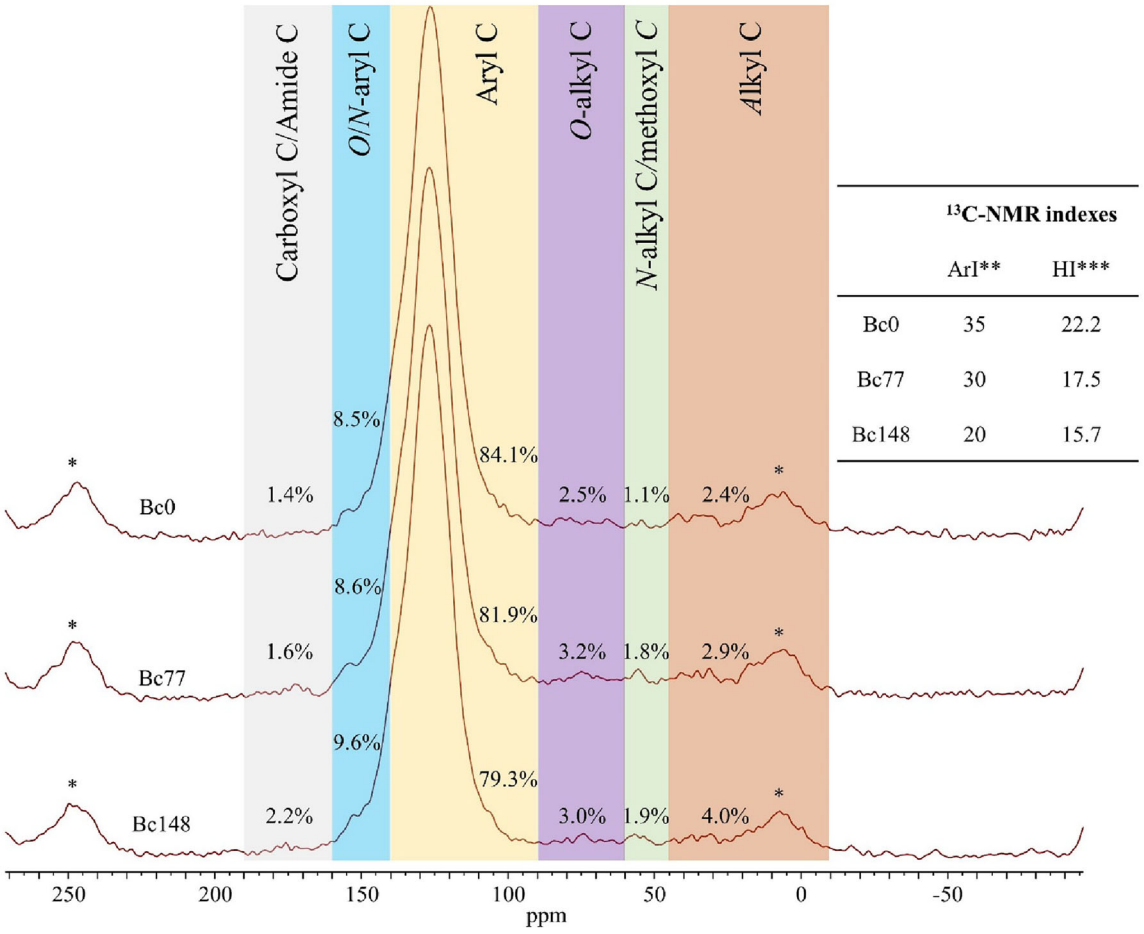

	^{13}C-NMR indexes	
	ArI**	HI***
Bc0	35	22.2
Bc77	30	17.5
Bc148	20	15.7

FIGURE 6 Solid state carbon-13 nuclear magnetic resonance (^{13}C-NMR) spectra with relative contribution (%) of carbon chemical groups to the total spectrum intensity, aromaticity index (ArI), and hydrophobicity index (HI) of original biochar (Bc0), biochar co-composted for 77 (Bc77) and 148 (Bc148) days. *Spinning side bands. **ArI = aryl C/alkyl C. ***HI = (aryl C + alkyl C)/(carboxyl C + O-alkyl C).

Bc, or lower in Bc. However, our research focus was on the relationships between N_{min} in biochar and N_2O emissions.

Nitrification started in the 4th week of composting, when compost temperature dropped below 45°C, allowing nitrifying bacteria and archaea to resume their activity in the compost (Sánchez-Monedero et al., 2001). The clear trend toward higher NH_4^+ content (mg N kg^{-1}) in Ctrl likely indicates possible strong retention of NH_4^+ by biochar or a reduced accumulation of NH_4^+ due to lower compost mass loss in Bc. This "dilution" effect was also noticed for P_{av} and K_{av} contents (Figure S4) and EC (Figure 2c). Contrarily, this was not noticed for NO_3^- contents. Instead, the similar NO_3^- contents in Ctrl and Bc, together with the higher amount of NO_3^- (g $pile^{-1}$) in Bc compared to Ctrl during composting, suggest that biochar acted as additional NO_3^- reservoir in compost (Agyarko-Mintah et al., 2017). This can occur via flow of NO_3^- from compost into biochar pores following a concentration gradient and subsequent blockage of biochar pores by organo-mineral layers formed during composting (Joseph et al., 2018). In Hagemann et al. (2017b), this was demonstrated by additional recovery of NO_3^- from biochar particles following successive extractions with 2 mol L^{-1} KCl, converging with our results. In our study, this was further supported by SEM-EDX, which revealed the deposition of organic material on biochar surface (Figure S5) and the appearance of minerals containing K, Si, P, S, and Cl on the expense of the carbon proportion (Table S1) after composting.

4.3 | Nitrogen dynamics in biochar particles

Biochar retained NH_4^+ despite its minimal functionalization (<2.2% carboxyl-C, Figure 6), suggesting that NH_4^+ might have been captured by biochar also via other mechanisms. Possibly, NH_4^+ concentrated in the initial compost moved into biochar pores, following a concentration gradient facilitated by the high MC of the initial compost. The recovery of NH_4^+ in the different extraction steps may indicate the involvement of different NH_4^+ retention mechanisms in biochar particles. Most of the NH_4^+ retained by biochar

within the first week of composting was extracted in Es1 and may have been released along the composting process and subjected to further transformations. Consequently, the concentration of NH_4^+ in Es1 decreased over time, while that extracted in Es3 remained practically unchanged during composting. Biochar particles not only retained NH_4^+, NO_2^-, and NO_3^-, but it can be hypothesized that nitrification may have occurred on the biochar surface, favored by the alkaline compost conditions. According to Y. Li et al. (2012), ferric oxides, which were present in our biochar ash (iron as Fe_2O_3 1.2%), could have led to further redox reactions and hence oxidation of NH_4^+ to NO_3^- at the biochar surface. This may explain the low NO_3^- content in Bc on day 48 and the increased NO_3^- contents extracted from biochar particles. After pile turning on day 41, followed by a clear increase of strongly retained NO_2^- content in the biochar (6.3 mg kg^{-1}, corresponding to 40.9% of NO_2^- retained in biochar, Figure 4c, 4d), the NH_4^+ content in Es1 decreased. Thus, it is plausible to assume that biochar-retained NH_4^+ was converted into NO_2^- during this period. Furthermore, the strong retention of NH_4^+ in biochar particles (Es3), together with a reduced mass loss in Bc, may explain the tendency of greater content of NH_4^+ in Ctrl compost (Figure 3c).

The minimal enrichment of biochar with carboxyl C through composting (Figure 6) indicates that the storage of strongly retained NO_3^- (194 mg N kg^{-1}) in biochar may result from entrapment of NO_3^--rich water in biochar pores and subsequent formation of an organo-mineral layer on top of the pores (Joseph et al., 2018), rather than by cation bridges between biochar carboxylic groups and NO_3^-. The high SSA of the biochar (Table 1) together with the moisture of the compost pile (mostly between 50% and 70%, Figure 2a) may have favored the transport of NO_3^- with water toward internal biochar pores. This is in line with Hagemann et al. (2017a), who found greater NO_3^- in co-composted biochar with greater SSA. Entrapment of NO_3^- in biochar pores may have been facilitated by organic coating of biochar due to biochar particles contact with compost, which reduces the hydrophobicity of biochar (Hagemann et al., 2017b). In our work this is supported by a gradual reduction of biochar HI with composting time (Figure 6).

4.4 | GHG emissions

Czekała et al. (2016) found that biochar increased CO_2 emissions from poultry manure compost by enhancing compost porosity and accelerating OM decomposition. Steiner et al. (2010) argued similarly to explain greater CO_2 emissions (28%) from poultry litter composting after biochar amendment at 20% (dw). Awasthi et al. (2017) found that CO_2 emissions from sewage sludge composting with WS increased with increasing biochar amendment rates (2% up to 18%), as gains in compost aeration depend on biochar amendment rate. This is also suggested by Sánchez-García et al. (2015), who found that low doses of biochar did not affect CO_2 emissions from manure composting. Based on these studies, seems the adequate mixture of WS, KS, and HM, together with compost pile turning and absence of excessive MC in our study already provided proper oxygenation of the pile, without additional aeration provided by biochar. This is in line with the lack of additional CO_2 emissions in Bc compared to Ctrl. Likewise, Sánchez-García et al. (2015) reported that biochar amendment at 3% to poultry litter and barley straw compost did not change CH_4 fluxes as biochar did not induce additional oxygenation of the compost, probably because the amendment rate was too low.

Emission of CH_4 from compost may originate from high O_2 consumption in early composting stages due to intensified microbial activity. Concomitantly, the breakdown of larger feedstock particles into smaller pieces may create anaerobic patches in the compost, intensifying anaerobic decomposition of OM by methanogenic organisms (Sánchez-García et al., 2015). Thus, several studies found mitigation of CH_4 emissions from compost after biochar amendment due to enhanced compost oxygenation (Chen et al., 2017; N. Liu et al., 2017; Q. Wang et al., 2018). Sonoki et al. (2013) found that biochar-amended (10%) compost exhibited levels of methanogenic organisms twofold lower compared to the control, while the level of methanotrophic organisms was threefold higher. In our study, CH_4 emissions occurred possibly due to high initial compost MC leading to formation of anaerobic spots. However, as CH_4 emissions in Ctrl and Bc did not differ, it seems that anaerobic patches formed in the compost independently on the presence of biochar.

Several studies found that biochar reduced N_2O emissions from compost (Agyarko-Mintah et al., 2017; S. Li et al., 2016; Q. Wang et al., 2018). In our study, biochar did not affect N_2O emissions. However, N_2O emission tended to peak higher in Ctrl compared to Bc after pile turning (day 41), possibly in response to reduction of N available in compost for N_2O formation. For instance, a significant amount of NH_4^+ was strongly bound to biochar on day 43 (Figure 4a). This N_2O emission peak is likely attributed to nitrification, as compost NO_3^- contents increased shortly afterward. As compost parameters strongly governing N_2O emissions, as MC, temperature, NO_3^-–N, and NH_4^+–N content were not affected by biochar, remarkable effects of biochar on N_2O emissions may have been prevented.

The N_2O emissions measured in this experiment (peak emissions of 36.1–83.3 mg N_2O-N m^{-2} day^{-1}) were significantly lower compared to that reported by Castro-Herrera et al. (2023) for human and cattle manure composted with or without biochar (198–789 mg N_2O-N m^{-2} day^{-1}). In their study, the manure NH_4^+ contents were 10-fold higher compared to the present study, which probably led to N_2O

emissions of greater magnitude. S. Li et al. (2016) reported even higher peak emissions (613–3568 mg N_2O m^{-2} day^{-1}) for windrow composting of cattle manure and rice straw. These authors assigned biochar-mediated N_2O emission mitigations to N_{min} capture by biochar, but without monitoring this explicitly. Even though biochar captured significant amounts of NH_4^+ and NO_3^- and reduced the GWP of compost by 8% in our study, this reduction was not statistically significant compared to Ctrl. The main pathway for N_2O production in our work is proposed to be the autotrophic nitrification, likely favored by the similar alkaline pH (along most of composting course) in Ctrl and Bc compost. Duan et al. (2019) observed N_2O emission mitigation after biochar amendment (40 Mg ha^{-1}) to an alkaline soil. This was later attributed to reduction of the abundance of ammonia-oxidizing bacteria in soil induced by biochar and retention of NH_4^+ by biochar carboxyl and hydroxyl groups (Fan et al., 2020). In our work, cumulative N_2O emission mitigation by biochar was not demonstrated, suggesting that such biochar-associated mechanisms were not clearly present, possibly because of the lower rate of biochar amendment to compost and the lower abundance of cation exchange sites of the biochar in our work. Similar to our work, H. Wang et al. (2021) and Castro-Herrera et al. (2023) did not find differences between the GWP of compost with or without biochar. However, differently from our work, where biochar did not alter CO_2, CH_4, and N_2O cumulative emissions, the authors found that greater emissions of one GHG were offset by reduced emissions of other GHG.

4.5 | Changes in biochar chemical structure with composting time

The ^{13}C-NMR spectra of Bc0, Bc77, and Bc148 (Figure 6) are typical of woody feedstock-derived biochar produced at high pyrolysis temperatures (Cao et al., 2012) and revealed minimal enrichment of biochar with carboxyl C (functionalization) through composting. According to Hilscher and Knicker (2011), the oxidation of aryl C occurs in two steps. First, aromatic C is modified microbiologically by substitution with OH-groups to form catechol-like compounds, then cleavage of O-aryl C rings occurs leading to enrichment in carboxyl C groups. In fact, this is evidenced by the gradual increase of the carboxyl C + O/N-aryl C/aryl C ratio with composting time: Bc0 (0.12), Bc77 (0.13), and Bc148 (0.15). However, these chemical shifts were still minimal, probably due to the high aromaticity of the biochar used in the experiment, which enhances its resistance against biodegradation (L. Wang et al., 2022). In our study, the reduction in biochar aromaticity with composting time is accompanied by an enrichment of alkyl C rather than of carboxyl C (i.e., gains in cation exchange capacity). The magnitude of the chemical shifts in the biochar observed in our study is quite comparable to that reported by De la Rosa et al. (2018) for sewage-sludge-derived biochar produced at 600°C and aged in soil for 120 days. The authors observed that aging of biochar reduced the aryl C signal from 58% to 51% and increased the alkyl C signal from 7% to 12%. This was attributed to fungi colonization of biochar pores leading to degradation of aromatic structures and increase in alkyl C forms in the biochar. Consequently, the authors found that the aromaticity index of the original biochar was 1.8-fold greater compared to the aged biochar, which is comparable to values found in the present study (1.7-fold) when comparing Bc0 and Bc148. Furthermore, the authors observed minimal carboxyl C enrichment in biochar after aging (1%), as similarly found in the present study (0.8%).

5 | CONCLUSIONS

In our experiment, biochar did not change compost temperature, MC, and pH, which are known to govern CO_2, CH_4, and N_2O fluxes. Apparently, compost feedstocks were well balanced and, together with pile turning, provided proper conditions for aerobic composting. Thus, an increase in CO_2 or decrease in CH_4 and N_2O emissions from compost associated with an increase in compost oxygenation after biochar amendment was not evident in our work. We demonstrated that biochar retained considerable amounts of NH_4^+, mainly at early composting stages, and NO_3^- mainly at later composting stages, both in easily extractable and strongly retained forms, despite the minimal abundance of carboxyl C in the biochar structure, without reducing N_2O emissions, contrary to our hypothesis. Overall, composting local and easily available feedstock with biochar enhanced the recovery of NO_3^- compost without stimulating GHG emissions.

AUTHOR CONTRIBUTIONS

Franziska Busch: Data curation; formal analysis; investigation; methodology; visualization; writing—original draft; writing—review and editing. **Otávio dos Anjos Leal**: Conceptualization; data curation; formal analysis; investigation; methodology; supervision; visualization; writing—original draft; writing—review and editing. **Nina Siebers**: Data curation; formal analysis; methodology; visualization; writing—original draft; writing—review and editing. **Nicolas Brüggemann**: Conceptualization; investigation; methodology; supervision; visualization; writing—original draft; writing—review and editing.

ACKNOWLEDGMENTS

Special thanks go to Dr. Katharina Prost for valuable discussions prior to the installation of the experiment, to Lina Rohlmann for helping to organize feedstocks pick up, and

to the laboratory technicians Franz Leistner, Holger Wissel, and Sirgit Kummer. The authors also thank the companies Burgmühle and Stütgerhof for providing the kitchen scraps and horse manure, respectively, free of charge. This research was financially supported by the Bioeconomy Science Center's NewBIAS project. The scientific activities of the Bioeconomy Science Center were financially supported by the Ministry of Culture and Science of the Federal State of North Rhine-Westphalia (NRW), Germany, within the framework of the NRW Strategieprojekt BioSC (No. 313/323-400-00213).

Open access funding enabled and organized by Projekt DEAL.

CONFLICT OF INTEREST STATEMENT

The authors declare no conflicts of interest.

ORCID

Franziska Busch https://orcid.org/0009-0008-6212-8364
Otávio dos Anjos Leal https://orcid.org/0000-0003-2786-4119
Nina Siebers https://orcid.org/0000-0002-6431-0046
Nicolas Brüggemann https://orcid.org/0000-0003-3851-2418

REFERENCES

Agyarko-Mintah, E., Cowie, A., Singh, B. P., Joseph, S., van Zwieten, L., Cowie, A., Harden, S., & Smillie, R. (2017). Biochar increases nitrogen retention and lowers greenhouse gas emissions when added to composting poultry litter. *Waste Management*, *61*, 138–149. https://doi.org/10.1016/j.wasman.2016.11.027

Ajibade, S., Nnadozie, E. C., Iwai, C. B., Ghotekar, S., Chang, S. W., Ravindran, B., & Kumar Awasthi, M. K. (2023). Biochar-based compost: A bibliometric and visualization analysis. *Bioengineered*, *13*(7–12), 15013–15032. https://doi.org/10.1080/21655979.2023.2177369

Akdeniz, N. (2019). A systematic review of biochar use in animal waste composting. *Waste Management*, *88*, 291–300. https://doi.org/10.1016/j.wasman.2019.03.054

Awasthi, M. K., Wang, M., Chen, H., Wang, Q., Zhao, J., Ren, X., Li, D.-S., Awasthi, S. K., Shen, F., Li, R., & Zhang, Z. (2017). Heterogeneity of biochar amendment to improve the carbon and nitrogen sequestration through reduce the greenhouse gases emissions during sewage sludge composting. *Bioresource Technology*, *224*, 428–438. https://doi.org/10.1016/j.biortech.2016.11.014

Beck-Friis, B., Smårs, S., Jönsson, H., & Kirchmann, H. (2001). SE—Structures and environment. *Journal of Agricultural Engineering Research*, *78*(4), 423–430. https://doi.org/10.1006/jaer.2000.0662

Bernal, M. P., Alburquerque, J. A., & Moral, R. (2009). Composting of animal manures and chemical criteria for compost maturity assessment. A review. *Bioresource Technology*, *100*(22), 5444–5453. https://doi.org/10.1016/j.biortech.2008.11.027

Bouwman, L., Goldewijk, K. K., van der Hoek, K. W., Beusen, A. H. W., van Vuuren, D. P., Willems, J., Rufino, M. C., & Stehfest, E. (2013). Exploring global changes in nitrogen and phosphorus cycles in agriculture induced by livestock production over the 1900–2050 period. *Proceedings of the National Academy of Sciences of the United States of America*, *110*(52), 20882–20887. https://doi.org/10.1073/pnas.1012878108

Bundesministerium der Justiz und für Verbraucherschutz. (2022). *Verordnung über die Ver-wertung von Bioabfällen auf landwirtschaftlich, forstwirtschaftlich und gärtnerisch genutzten Böden (Bioabfallverordnung–BioAbfV): BioAbfV*. Bundesministerium der Justiz und für Verbraucherschutz. http://www.gesetze-im-internet.de/bioabfv/index.html

Cáceres, R., Malińska, K., & Marfà, O. (2018). Nitrification within composting: A review. *Waste Management*, *72*, 119–137. https://doi.org/10.1016/j.wasman.2017.10.049

Canadell, J., Monteiro, P., Costa, M., Da Cotrim Cunha, L., Cox, P., Eliseev, A. V., Henson, S., Ishii, M., Jaccard, S., Koven, C., Lohila, A., Patra, P. K., Piao, S., Rogelj, J., Syampungani, S., Zaehle, S., & Zickfeld, K. (2021). Global carbon and other biogeochemical cycles and feedbacks. In V. Masson-Delmotte (Ed.), *Climate change 2021: The physical science basis. Contribution of working group I to the sixth assessment report of the Intergovernmental Panel on Climate Change* (pp. 673–816). Cambridge University Press. https://doi.org/10.1017/9781009157896.007

Cao, X., Pignatello, J. J., Li, Y., Lattao, C., Chappell, M. A., Chen, N., Miller, L. F., & Mao, J. (2012). Characterization of wood chars produced at different temperatures using advanced solid-state ^{13}C NMR spectroscopic techniques. *Energy & Fuels*, *26*(9), 5983–5991. https://doi.org/10.1021/ef300947s

Castro-Herrera, D., Prost, K., Schäfer, Y., Kim, D.-G., Yimer, F., Tadesse, M., Gebrehiwot, M., & Brüggemann, N. (2022). Nutrient dynamics during composting of human excreta, cattle manure, and organic waste affected by biochar. *Journal of Environmental Quality*, *51*(1), 19–32. https://doi.org/10.1002/jeq2.20312

Castro-Herrera, D., Prost, K., Kim, D.-G., Yimer, F., Tadesse, M., Gebrehiwot, M., & Brüggemann, N. (2023). Biochar addition reduces non-CO_2 greenhouse gas emissions during composting of human excreta and cattle manure. *Journal of Environmental Quality*, *52*(4), 814–828. https://doi.org/10.1002/jeq2.20482

Chen, W., Liao, X., Wu, Y., Liang, J. B., Mi, J., Huang, J., Zhang, H., Wu, Y., Qiao, Z., Li, X., & Wang, Y. (2017). Effects of different types of biochar on methane and ammonia mitigation during layer manure composting. *Waste Management*, *61*, 506–515. https://doi.org/10.1016/j.wasman.2017.01.014

Czekała, W., Malińska, K., Cáceres, R., Janczak, D., Dach, J., & Lewicki, A. (2016). Co-composting of poultry manure mixtures amended with biochar—The effect of biochar on temperature and C-CO_2 emission. *Bioresource Technology*, *200*, 921–927. https://doi.org/10.1016/j.biortech.2015.11.019

De La Rosa, J., Miller, A. Z., & Knicker, H. (2018). Soil-borne fungi challenge the concept of long-term biochemical recalcitrance of pyrochar. *Scientific Reports*, *8*(1), Article 2896. https://doi.org/10.1038/s41598-018-21257-5

Duan, P., Zhou, J., Feng, L., Jansen-Willems, A. B., & Xiong, Z. (2019). Pathways and controls of N_2O production in greenhouse vegetable production soils. *Biology and Fertility of Soils*, *55*, 285–297. https://doi.org/10.1007/s00374-019-01348-9

European Biochar Foundation. (2012). *European biochar certificate—Guidelines for a sustainable production of biochar (Version 9.4E)*. European Biochar Foundation. https://www.european-biochar.org/media/doc/2/version_en_9_4.pdf

Fan, C., Duan, P., Zhang, X., Shen, H., Chen, M., & Xiong, Z. (2020). Mechanisms underlying the mitigation of both N2O and NO emissions with field-aged biochar in an Anthrosol. *Geoderma*, *364*, 114178. https://doi.org/10.1016/j.geoderma.2020.114178

FAO. (2008). *Guide to laboratory establishment for plant nutrient analysis (FAO fertilizer and plant nutrition)* (Bulletin No. TC[M/I0131E/1/07.08/1100]). Food and Agriculture Organization of the United Nations.

Firmino, M. V., & Trémier, A. (2023). Nitrogen losses mitigation by supplementing composting mixture with biochar: Research of the ruling parameters. *Waste and Biomass Valorization*, *15*, 959–971. https://doi.org/10.1007/s12649-023-02204-6

Fischer, D., & Glaser, B. (2012). Synergisms between compost and biochar for sustainable soil amelioration. In S. Kumar & A. Bharti (Eds.), *Management of organic waste* (pp. 167–198). IntechOpen. https://doi.org/10.5772/31200

Fowler, D., Coyle, M., Skiba, U., Sutton, M. A., Cape, J. N., Reis, S., Sheppard, L. J., Jenkins, A., Grizzetti, B., Galloway, J. N., Vitousek, P., Leach, A., Bouwman, A. F., Butterbach-Bahl, K., Dentener, F., Stevenson, D., Amann, M., & Voss, M. (2013). The global nitrogen cycle in the twenty-first century. *Philosophical Transactions of the Royal Society B: Biological Sciences*, *368*(1621), 20130164. https://doi.org/10.1098/rstb.2013.0164

Hagemann, N., Joseph, S., Schmidt, H.-P., Kammann, C. I., Harter, J., Borch, T., Young, R. B., Varga, K., Taherymoosavi, S., Elliott, K. W., McKenna, A., Albu, M., Mayrhofer, C., Obst, M., Conte, P., Dieguez-Alonso, A., Orsetti, S., Subdiaga, E., Behrens, S., & Kappler, A. (2017). Organic coating on biochar explains its nutrient retention and stimulation of soil fertility. *Nature Communications*, *8*(1), Article 1089. https://doi.org/10.1038/s41467-017-01123-0

Hagemann, N., Kammann, C. I., Schmidt, H. P., Kappler, A., & Behrens, S. (2017). Nitrate capture and slow release in biochar amended compost and soil. *PloS One*, *12*(2), e0171214. https://doi.org/10.1371/journal.pone.0171214

Hagemann, N., Subdiaga, E., Orsetti, S., de La Rosa, J. M., Knicker, H., Schmidt, H.-P., Kappler, A., & Behrens, S. (2018). Effect of biochar amendment on compost organic matter composition following aerobic composting of manure. *Science of the Total Environment*, *613–614*, 20–29. https://doi.org/10.1016/j.scitotenv.2017.08.161

Haider, G., Steffens, D., Müller, C., & Kammann, C. I. (2016). Standard extraction methods may underestimate nitrate stocks captured by field-aged biochar. *Journal of Environmental Quality*, *45*(4), 1196–1204. https://doi.org/10.2134/jeq2015.10.0529

Haider, G., Joseph, S., Steffens, D., Müller, C., Taherymoosavi, S., Mitchell, D., & Kammann, C. I. (2020). Mineral nitrogen captured in field-aged biochar is plant-available. *Scientific Reports*, *10*(1), Article 13816. https://doi.org/10.1038/s41598-020-70586-x

He, X., Chen, L., Han, L., Liu, N., Cui, R., Yin, H., & Huang, G. (2017). Evaluation of biochar powder on oxygen supply efficiency and global warming potential during mainstream largescale aerobic composting. *Bioresource Technology*, *245*, 309–317. https://doi.org/10.1016/j.biortech.2017.08.076

Hilscher, A., & Knicker, H. (2011). Degradation of grass-derived pyrogenic organic material, transport of the residues within a soil column and distribution in soil organic matter fractions during a 28 month microcosm experiment. *Organic Geochemistry*, *42*(1), 42–54. https://doi.org/10.1016/j.orggeochem.2010.10.005

IPCC. (2021). *Climate change 2021: The physical science basis. Contribution of working group I to the sixth assessment report of the intergovernmental panel on climate change* [V. Masson-Delmotte, P. Zhai, A. Pirani, S. L. Connors, C. Péan, S. Berger, N. Caud, Y. Chen, L. Goldfarb, M. I. Gomis, M. Huang, K. Leitzell, E. Lonnoy, J. B. R. Matthews, T. K. Maycock, T. Waterfield, O. Yelekçi, R. Yu, & B. Zhou, Eds.]. Cambridge University Press. https://doi.org/10.1017/9781009157896

Jia, G., Shevliakova, E., Artaxo, P., De Noblet-Ducoudré, N., Houghton, R., House, J., Kitajima, K., Lennard, C., Popp, A., Sirin, A., Sukumar, R., & Verchot, L. (2019). Land–climate interactions. In P. R. Shukla et al. (Ed.), *Climate change and land: An IPCC special report on climate change, desertification, land degradation, sustainable land management, food security, and greenhouse gas fluxes in terrestrial* (pp. 131–248). Cambridge University Press. https://doi.org/10.1017/9781009157988.004

Joseph, S., Kammann, C. I., Shepherd, J. G., Conte, P., Schmidt, H.-P., Hagemann, N., Rich, A. M., Marjo, C. E., Allen, J., Munroe, P., Mitchell, D. R. G., Donne, S., Spokas, K., & Graber, E. R. (2018). Microstructural and associated chemical changes during the composting of a high temperature biochar: Mechanisms for nitrate, phosphate and other nutrient retention and release. *Science of the Total Environment*, *618*, 1210–1223. https://doi.org/10.1016/j.scitotenv.2017.09.200

Kammann, C. I., Schmidt, H.-P., Messerschmidt, N., Linsel, S., Steffens, D., Müller, C., Koyro, H.-W., Conte, P., & Joseph, S. (2015). Plant growth improvement mediated by nitrate capture in co-composted biochar. *Scientific Reports*, *5*, Article 11080. https://doi.org/10.1038/srep11080

Kammann, C., Glaser, B., & Schmidt, H.-P. (2016). Combining biochar and organic amendments. In B. Glaser, G. Ruysschaert, K. Zwart, & S. Shackley (Ed.), *Biochar in European soils and agriculture: Science and practice* (pp.136–160). Routledge.

Khan, N., Clark, I., Sánchez-Monedero, M. A., Shea, S., Meier, S., & Bolan, N. (2014). Maturity indices in co-composting of chicken manure and sawdust with biochar. *Bioresource Technology*, *168*, 245–251. https://doi.org/10.1016/j.biortech.2014.02.123

Knicker, H., Totsche, K. U., Almendros, G., & González-Vila, F. J. (2005). Condensation degree of burnt peat and plant residues and the reliability of solid-state VACP MAS ^{13}C NMR spectra obtained from pyrogenic humic material. *Organic Geochemistry*, *36*(10), 1359–1377. https://doi.org/10.1016/j.orggeochem.2005.06.006

Lasaridi, K., Protopapa, I., Kotsou, M., Pilidis, G., Manios, T., & Kyriacou, A. (2006). Quality assessment of composts in the Greek market: The need for standards and quality assurance. *Journal of Environmental Management*, *80*(1), 58–65. https://doi.org/10.1016/j.jenvman.2005.08.011

Lehmann, J., Cowie, A., Masiello, C. A., Kammann, C., Woolf, D., Amonette, J. E., Cayuela, M. L., Camps-Arbestain, M., & Whitman, T. (2021). Biochar in climate change mitigation. *Nature Geoscience*, *14*(12), 883–892. https://doi.org/10.1038/s41561-021-00852-8

Li, Y., Yu, S., Strong, J., & Wang, H. (2012). Are the biogeochemical cycles of carbon, nitrogen, sulfur, and phosphorus driven by the "FeIII–FeII redox wheel" in dynamic redox environments? *Journal of Soils and Sediments*, *12*(5), 683–693. https://doi.org/10.1007/s11368-012-0507-z

Li, R., Wang, Q., Zhang, Z., Zhang, G., Li, Z., Wang, L., & Zheng, J. (2015). Nutrient transformation during aerobic composting of pig manure with biochar prepared at different temperatures. *Environmental Technology*, *36*(5–8), 815–826. https://doi.org/10.1080/09593330.2014.963692

Li, S., Song, L., Jin, Y., Liu, S., Shen, Q., & Zou, J. (2016). Linking N_2O emission from biochar amended composting process to the abundance of denitrify (nirK and nosZ) bacteria community. *AMB Express*, *6*(1), Article 37. https://doi.org/10.1186/s13568-016-0208-x

Liu, N., Zhou, J., Han, L., Ma, S., Sun, X., & Huang, G. (2017). Role and multi-scale characterization of bamboo biochar during poultry manure aerobic composting. *Bioresource Technology*, *241*, 190–199. https://doi.org/10.1016/j.biortech.2017.03.144

Liu, Q., Zhang, Y., Liu, B., Amonette, J. E., Lin, Z., Liu, G., Ambus, P., & Xie, Z. (2018). How does biochar influence soil N cycle? A meta-analysis. *Plant and Soil*, *426*(1–2), 211–225. https://doi.org/10.1007/s11104-018-3619-4

Loganathan, P., Vigneswaran, S., & Kandasamy, J. (2013). Enhanced removal of nitrate from water using surface modification of adsorbents—A review. *Journal of Environmental Management*, *131*, 363–374. https://doi.org/10.1016/j.jenvman.2013.09.034

López-Cano, I., Roig, A., Cayuela, M. L., Alburquerque, J. A., & Sánchez-Monedero, M. A. (2016). Biochar improves N cycling during composting of olive mill wastes and sheep manure. *Waste Management*, *49*, 553–559. https://doi.org/10.1016/j.wasman.2015.12.031

Maheshwari, D. K. (2014). *Composting for sustainable agriculture* (Vol. 3). Springer International. https://doi.org/10.1007/978-3-319-08004-8

Nguyen, M. K., Lin, C., Hoang, H. G., Sanderson, P., Dang, B. T., Bui, X. T., Nguyen, N. S. H., Vo, D.-V. N., & Tran, H. T. (2022). Evaluate the role of biochar during the organic waste composting process: A critical review. *Chemosphere*, *299*, 134488. https://doi.org/10.1016/j.chemosphere.2022.134488

Prost, K., Borchard, N., Siemens, J., Kautz, T., Séquaris, J.-M., Möller, A., & Amelung, W. (2013). Biochar affected by composting with farmyard manure. *Journal of Environmental Quality*, *42*(1), 164–172. https://doi.org/10.2134/jeq2012.0064

UBA. (2020). *Nährstoffeinträge aus der Landwirtschaft und Stickstoffüberschuss*. https://www.umweltbundesamt.de/daten/land-forstwirtschaft/naehrstoffeintraege-aus-der-landwirtschaft

Rynk, R., van de Kamp, M., Willson, G. B., Singley, M. E., Richard, T. L., Kolega, J. J., Gouin, F., Laliberty, L., Kay, D., Murphy, D., Hoitink, H., & Brinton, W. F. (1992). On-farm composting handbook. *Northeast Regional Agricultural Engineering Service*, *152*, 14853–5701. https://ecommons.cornell.edu/handle/1813/67142

Sánchez-García, M., Alburquerque, J. A., Sánchez-Monedero, M. A., Roig, A., & Cayuela, M. L. (2015). Biochar accelerates organic matter degradation and enhances N mineralisation during composting of poultry manure without a relevant impact on gas emissions. *Bioresource Technology*, *192*, 272–279. https://doi.org/10.1016/j.biortech.2015.05.003

Sánchez-Monedero, M. A., Roig, A., Paredes, C., & Bernal, M. P. (2001). Nitrogen transformation during organic waste composting by the Rutgers system and its effects on pH, EC and maturity of the composting mixtures. *Bioresource Technology*, *78*(3), 301–308. https://doi.org/10.1016/S0960-8524(01)00031-1

Sánchez-Monedero, M. A., Cayuela, M. L., Roig, A., Jindo, K., Mondini, C., & Bolan, N. (2018). Role of biochar as an additive in organic waste composting. *Bioresource Technology*, *247*, 1155–1164. https://doi.org/10.1016/j.biortech.2017.09.193

Schäfer, Y. (2020). *Impact of biochar on nutrient dynamics during composting of humanure, cattle manure and other organic materials–-A case study from South Ethiopia* [Master's thesis, University of Bonn].

Schmidt, H. P., Kammann, C., Hagemann, N., Leifeld, J., Bucheli, T. D., Sánchez-Monedero, M. A., & Cayuela, M. L. (2021). Biochar in agriculture—A systematic review of 26 global meta-analyses. *GCB Bioenergy*, *13*(11), 1708–1730. https://doi.org/10.1111/gcbb.12889

Sonoki, T., Furukawa, T., Jindo, K., Suto, K., Aoyama, M., & Sánchez-Monedero, M. Á. (2013). Influence of biochar addition on methane metabolism during thermophilic phase of composting. *Journal of Basic Microbiology*, *53*(7), 617–621. https://doi.org/10.1002/jobm.201200096

Steiner, C., Das, K. C., Melear, N., & Lakly, D. (2010). Reducing nitrogen loss during poultry litter composting using biochar. *Journal of Environmental Quality*, *39*(4), 1236–1242. https://doi.org/10.2134/jeq2009.0337

VDLUFA. (2008). *Methodenbuch Band II.2. Die Untersuchung von Sekundärrohstoffdüngern, Kultursubstraten und Bödenhilfsstoffen: Bestimmung von Phosphor und Kalium im Calcium-Acetat-Lactat-Auszug*. VDLUFA.

VDLUFA. (2014). *Methodenbuch Band II.2. Die Untersuchung von Sekundärrohstoff-düngern, Kultursubstraten und Bödenhilfsstoffen: Bestimmung des wesentlichen Geh-altes an verfügbarem Stickstoff (Ammonium und Nitrat): $CaCl_2$-Auszug*. VDLUFA.

Wang, Y., Lin, Y., Chiu, P. C., Imhoff, P. T., & Guo, M. (2015). Phosphorus release behaviors of poultry litter biochar as a soil amendment. *Science of the Total Environment*, *512–513*, 454–463. https://doi.org/10.1016/j.scitotenv.2015.01.093

Wang, Q., Awasthi, M. K., Ren, X., Zhao, J., Li, R., Wang, Z., Wang, M., Chen, H., & Zhang, Z. (2018). Combining biochar, zeolite and wood vinegar for composting of pig manure: The effect on greenhouse gas emission and nitrogen conservation. *Waste Management*, *74*, 221–230. https://doi.org/10.1016/j.wasman.2018.01.015

Wang, H., Lu, Y., Xu, J., Liu, X., & Sheng, L. (2021). Effects of additives on nitrogen transformation and greenhouse gases emission of co-composting for deer manure and corn straw. *Environmental Science and Pollution Research International*, *28*(10), 13000–13020. https://doi.org/10.1007/s11356-020-11302-0

Wang, L., Olsen, M. N., Moni, C., Dieguez-Alonso, A., de La Rosa, J. M., Stenrød, M., Liu, X., & Mao, L. (2022). Comparison of properties of biochar produced from different types of lignocellulosic biomass by slow pyrolysis at 600˚C. *Applications in Energy and Combustion Science*, *12*, 100090. https://doi.org/10.1016/j.jaecs.2022.100090

Wang, Y., Villamil, M. B., Davidson, P. C., & Akdeniz, N. (2019). A quantitative understanding of the role of co-composted biochar in plant growth using meta-analysis. *Science of the Total Environment*, *685*, 741–752. https://doi.org/10.1016/j.scitotenv.2019.06.244

Wang, N., He, Y., Zhao, K., Lin, X., He, X., Chen, A., Wu, G., Zhang, J., Yan, B., Luo, L., & Xu, D. (2024). Greenhouse gas emission characteristics and influencing factors of agricultural waste composting process: A review. *Journal of Environmental Management*, *354*, 120337. https://doi.org/10.1016/j.jenvman.2024.120337

Yang, B., Ma, Y., & Xiong, Z. (2019). Effects of different composting strategies on methane, nitrous oxide, and carbon dioxide emissions and nutrient loss during small-scale anaerobic composting. *Environmental Science and Pollution Research*, *26*(1), 446–455. https://doi.org/10.1007/s11356-018-3646-y

Yin, Y., Yang, C., Li, M., Zheng, Y., Ge, C., Gu, J., Li, H., Duan, M., Wang, X., & Chen, R. (2021). Research progress and prospects for using biochar to mitigate greenhouse gas emissions during composting: A review. *Science of The Total Environment*, *798*, 149294. https://doi.org/10.1016/j.scitotenv.2021.149294

Yuan, J., Chadwick, D., Zhang, D., Li, G., Chen, S., Luo, W., Du, L., He, S., & Peng, S. (2016). Effects of aeration rate on maturity and gaseous emissions during sewage sludge composting. *Waste Management*, *56*, 403–410. https://doi.org/10.1016/j.wasman.2016.07.017

Zhang, H., Marchant-Forde, J. N., Zhang, X., & Wang, Y. (2020). Effect of cornstalk biochar immobilized bacteria on ammonia reduction in laying hen manure composting. *Molecules*, *25*(7), 1560. https://doi.org/10.3390/molecules25071560

Zhou, S., Jiang, Z., Shen, J., Yao, Q., Yang, X., Li, X., Awasthi, M. K., & Zhang, Z. (2023). Biochar-amended compost as a promising soil amendment for enhancing plant productivity: A meta-analysis study. *Science of The Total Environment*, *879*, 163067. https://doi.org/10.1016/j.scitotenv.2023.163067

Zucconi, F. (1981). Evaluating toxicity of immature compost. *BioCycle*, 54–57. https://cir.nii.ac.jp/crid/1571135650109373312

SUPPORTING INFORMATION

Additional supporting information can be found online in the Supporting Information section at the end of this article.

How to cite this article: Busch, F., Leal, O. A., Siebers, N., & Brüggemann, N. (2024). Biochar captures ammonium and nitrate in easily extractable and strongly retained form without stimulating greenhouse gas emissions during composting. *Journal of Environmental Quality*, *53*, 1099–1115. https://doi.org/10.1002/jeq2.20634